

What Controls the Low Ice Number Concentration in the Upper Troposphere?

C. Zhou¹, J. E. Penner¹, G. Lin^{1*}, X. Liu² and M. Wang^{3, 4}

(1){University of Michigan, Ann Arbor, MI, USA}

(2){University of Wyoming, Laramie, WY, USA}

(3) {Institute for Climate and Global Change Research & School of Atmospheric Sciences, Nanjing University, Nanjing, 210023, China}

(4) {Collaborative Innovation Center of Climate Change, Jiangsu Province, China}

(*){now at: Pacific Northwest National Laboratory, Richland, Washington, USA}

Correspondence to: C. Zhou (zhouc@umich.edu)

Abstract

Cirrus clouds in the tropical tropopause play a key role in regulating the moisture entering the stratosphere through their dehydrating effect. Low ice number concentrations ($<200 \text{ L}^{-1}$) and high supersaturations (150-160%) have been observed in these clouds. Different mechanisms have been proposed to explain these low ice number concentrations, including the inhibition of homogeneous freezing by the deposition of water vapour onto pre-existing ice crystals, heterogeneous ice formation on glassy organic aerosol ice nuclei (IN), and limiting the formation of ice number from high frequency gravity waves. In this study, we examined the effect from three different representations of updraft velocities, the effect from pre-existing ice crystals, the effect from different water vapour deposition coefficients ($\alpha=0.1$ or 1), and the effect of 0.1% of the total secondary organic aerosol (SOA) particles acting as IN. Model simulated ice crystal numbers are compared against an aircraft observational dataset.

Including the effect from water vapour deposition on pre-existing ice particles can effectively reduce simulated in-cloud ice number concentrations for all model set-ups. A larger water vapour deposition coefficient ($\alpha=1$) can also efficiently reduce ice number concentrations at temperatures below 205K but less so at higher temperatures. SOA acting as

IN are most effective at reducing ice number concentrations when the effective updraft velocities are moderate ($\sim 0.05\text{--}0.2\text{ m s}^{-1}$). However, the effects of including SOA as IN and using ($\alpha=1$) are diminished when the effect from pre-existing ice is included.

When a grid resolved large-scale updraft velocity ($<0.1\text{ m s}^{-1}$) is used, the ice nucleation parameterization with homogeneous freezing only or with both homogeneous freezing and heterogeneous nucleation is able to generate low ice number concentrations in good agreement with observations for temperatures below 205K as long as the pre-existing ice effect is included. For the moderate updraft velocity ($\sim 0.05\text{--}0.2\text{ m s}^{-1}$) simulated ice number concentrations in good agreement with observations at temperatures below 205K can be achieved if effects from pre-existing ice, a larger water vapour deposition coefficient ($\alpha=1$) and SOA IN are all included. Using the sub-grid scale turbulent kinetic energy based updraft velocity ($\sim 0\text{--}2\text{ m s}^{-1}$) always overestimates the ice number concentrations at temperatures below 205K but compares well with observations at temperatures above 205K when the pre-existing ice effect is included.

1 Introduction

Cirrus clouds ($T < 35\text{ }^{\circ}\text{C}$) cover about a large fraction of the Earth's area from more than 10% to more than 30% depending on observational times, techniques and different thresholds of detectable optical depth (Wang et al., 1996; Rossow and Schiffer, 1999; Wylie and Menzel, 1999; Stubenrauch et al. 2000; Sassen et al., 2008) and are important in maintaining the global radiation balance (Ramanathan and Collins, 1991). They warm the atmosphere by absorbing outgoing longwave radiation emitted by the Earth and atmosphere and re-emitting it at much lower temperatures. This warming effect is partly compensated by their reflection of incoming solar radiation (Chen et al. 2000; IPCC 2013). Cirrus clouds also control the dehydration of air before its entry into the stratosphere (Jensen et al., 1996, 2013). Their radiative impacts, ability to affect water vapour cycles, and cirrus cloud evolution are sensitive to the ice number concentration. Ice in cirrus clouds can form through either homogeneous freezing of supercooled aqueous solutions (Koop et al. 2000) which typically generates high ice number concentrations or heterogeneous nucleation of different modes (deposition, contact, immersion, and condensation) triggered by insoluble aerosol particles (which are termed heterogeneous ice nuclei (IN)) (Pruppacher and Klett, 1997).

1 Heterogeneous nucleation typically forms much lower ice number concentrations due to the
2 limited IN concentration in the atmosphere (Rogers et al. 1998).

3 Low ice number concentrations ($<200 \text{ L}^{-1}$) and high in-cloud ice supersaturations (RH_i)
4 (150-160%) are frequently observed near the tropical tropopause layer (TTL) (e.g. Krämer et
5 al., 2009; Jensen et al. 2010, 2013). The observed high in-cloud ice supersaturations are
6 consistent with the long relaxation times needed to remove the excess water vapour above ice
7 saturation by deposition due to low ice number concentrations. These low ice numbers are not
8 consistent with the conventional theory of ice nucleation via homogenous freezing at the cold
9 temperatures in the TTL (e.g. Krämer et al., 2009; Jensen et al. 2010) if a typical value of
10 temperature fluctuation or updraft velocity is used.

11 Various proposals have been put forward to explain the low ice number concentrations in
12 the TTL. These can largely be divided into 3 categories. The first category is inhibition of
13 homogeneous freezing by heterogeneous IN (e.g. Abbatt et al. 2006; Murray et al. 2010) or
14 pre-existing ice particles (e.g. Kuebbeler et al. 2014; Shi et al. 2015). Abbatt et al. (2006)
15 showed that solid ammonium sulphate aerosols can be effective heterogeneous ice nuclei at
16 cirrus temperatures and lead to fewer but larger ice crystals compared to a homogeneous
17 freezing scenario. Murray et al. (2010) showed that organic matter can become glassy under
18 cirrus conditions and thereby become heterogeneous IN. Thus the low ice number and high
19 RH_i could be explained by heterogeneous nucleation of ice on glassy solution droplets.
20 Kuebbeler et al. (2014) studied the effect of vapour deposition onto pre-existing ice during
21 nucleation, which can prevent high supersaturations and thereby prevent either homogeneous
22 or heterogeneous freezing from occurring. They found that the effect of pre-existing ice
23 together with heterogeneous nucleation on mineral dust particles can significantly reduce
24 global ice crystal number and mass. Shi et al. (2015) also found that the inclusion of vapour
25 deposition onto pre-existing ice during nucleation significantly reduces ice number
26 concentrations in cirrus clouds, especially at middle to high latitudes in the upper troposphere
27 (by a factor of ~ 10).

28 The second category of proposals that might explain the observed low ice number
29 concentrations in the TTL is related to gravity wave cycles (e.g. Spichtinger and Krämer
30 2013; Dinh et al. 2015). In most ice nucleation parameterizations, it is often assumed that the
31 relevant time scale for ice nucleation (i.e., a few minutes) is sufficiently short such that the
32 vertical velocity and associated adiabatic cooling rate remain constant (e.g. Liu and Penner,

2005; Krächer et al., 2006; Barahona and Nenes, 2008). For the above proposals in the second category to form low ice numbers ($<200 \text{ L}^{-1}$) the constant cooling rate or updraft velocity has to be low enough (several cm s^{-1}). However, vertical velocity measurements from the Interhemispheric Differences in Cirrus Properties From Anthropogenic Emissions (INCA) campaign indicate that updraft velocities higher than 0.2 m s^{-1} are often observed (Krächer and Ström, 2003). Spichtinger and Krämer (2013) studied the effect of the superposition of a slow large-scale updraft with a high-frequency, short wavelength gravity wave. Under these circumstances, the observed TTL low cirrus ice numbers could be explained by “classical” homogeneous ice nucleation. They show model simulations of homogenous freezing starting at the tip of the high frequency wave just before it is about to turn from an upward movement to a downward movement. Consequently the amount of time available for homogenous freezing event is substantially limited due to the downdraft, and hence the newly formed ice number from homogeneous freezing is also reduced. They suggest that large-scale models would reproduce their results just by using the large-scale updraft velocity in ice nucleation parameterizations. Dinh et al. (2015) studied homogeneous ice nucleation using a parcel model with observed temperature time series from balloon flights near the tropical tropopause. They showed that low ice number concentrations can also be obtained if the gravity wave perturbations produce a non-persistent cooling rate such that the absolute change in temperature remains small during ice nucleation events.

The third category of proposals that might explain the observed low ice number concentrations in the TTL is related to the sedimentation of ice particles (e.g. Barahona and Nenes 2011; Murphy 2014). Barahona and Nenes (2011) showed that the dynamical balance between new ice particle production and sedimentation can set the cirrus clouds into one of two “preferred” microphysical regimes based on the magnitude of the temperature fluctuations. For small temperature fluctuations, the balance between the formation of ice crystals from homogeneous freezing and sedimentation was able to explain low ice number concentrations, although this finding could not be confirmed in the study by Jensen et al. (2012). Murphy (2014) showed that random temperature fluctuations can generate an extremely wide range of ice number densities. Since the low number density ice crystals are also associated with larger sizes, they sediment quickly and sweep out a much larger volume than that of the high number density ice crystals that stay aloft. Thus the rare temperature trajectories that result in the lowest number densities are disproportionately important. They

1 suggest the low mean and median observed ice number concentrations are caused by aircraft
2 observations which usually measure low ice number density in this much larger volume.

3 In this study, we will examine the first two categories of proposals in a GCM to see if
4 we are able to generate low ice number concentrations consistent with observations. We will
5 not evaluate the third category related to ice sedimentation. Even though sedimentation of ice
6 is included in the GCM (CAM5 in this study) by applying the mass- and number-weighted
7 terminal fall speeds which are obtained by integration over the particle size distributions with
8 appropriate weighting by number concentration or mixing ratio (Morrison and Gettelman
9 2008), the vertical grid spacing (with 30 vertical layers) is not fine enough to capture the
10 observed narrow layers of high ice crystal number concentrations with low ice crystal number
11 concentration layers surrounding them (Jensen et al., 2013). For the first category of
12 proposals, we will examine the effect of pre-existing ice and secondary organic aerosols
13 (SOA) acting as IN. For the second category of proposals, we will examine three different
14 representations of sub-grid updraft velocities in the ice nucleation parameterizations. For the
15 first representation, we follow the suggestion by Spichtinger and Krämer (2013) and simply
16 use the large-scale updraft velocity predicted by the GCM in the ice nucleation
17 parameterization, excluding any effect from fast gravity waves. For the second representation,
18 we use the sub-grid scale updraft velocity based on the fitted meso-scale temperature
19 fluctuations from long-term aircraft temperature observations (Gary 2006, 2008). This sub-
20 grid scale updraft velocity was first introduced in a GCM by Wang and Penner (2010) and
21 further studied by Wang et al. (2014). Wang et al. (2014) showed that using this updraft
22 velocity produces a better hemispheric contrast in ice supersaturation compared to
23 observations. The third representation is the sub-grid scale updraft velocity based on the
24 modelled sub-grid scale turbulent kinetic energy (TKE) (Neale et al. 2012; Gettelman et al.
25 2010). As shown in Fig. 1, this updraft velocity has the largest range. We will also examine
26 the effect of using different mass accommodation coefficients (α) for water vapour deposition
27 on ice crystals. This coefficient is not well known but has a significant impact on the
28 predicted ice numbers (Zhang et al. 2013; Murphy 2014). Laboratory measurements support
29 values from 0.006 (Magee et al. 2006) to unity (Skrotzki et al. 2013). Skrotzki et al. (2013)
30 constrained the value in the range of 0.2-1 with the majority of other lab studies also
31 supporting a value > 0.1 (see Table 1 in Skrotzki et al. (2013)). Kay and Wood (2008) showed
32 that α is ≥ 0.1 for small ice crystals forming at high ice supersaturations, so the small value of
33 α ($=0.006$) from (Magee et al., 2006) may only be appropriate for large ice crystals or at low

ice supersaturations. In this study we test two values of α (0.1 and 1). The model and experiments are described in section 2. Model results are presented in section 3. Section 4 presents a summary and a short discussion.

2 Model and Experiments

2.1 Description of the coupled CAM5/IMPACT model

We used the coupled CAM5/IMPACT model in this study. The CAM5/IMPACT model embeds the University of Michigan IMPACT chemistry and aerosol transport model as a module inside the Community Atmosphere Model version 5.3 (CAM5) (Zhou and Penner 2014). CAM5 is the atmospheric component of the Community Earth System Model version 1.2 (CESM1.2). Readers are referred to Neale et al. (2012) and Liu et al. (2012a) for more model details. Here we briefly summarize the ice nucleation process. Observation-based studies (e.g., Diao et al. 2013, 2014, 2015) as well as modelling studies (e.g., Spichtinger and Gierens 2009) show that the evolution of cirrus clouds undergo different phases including a clear-sky phase, ice nucleation phase, growth phase and decaying phase. Diao et al. (2013) suggests that the ice nucleation phase is a short-lived transient event since only 3-4% of sampled events are in this phase. GCMs (CAM5 here) usually use the time step longer than the duration of an ice nucleation event (30 min here). Thus the ice nucleation process has to be parameterized. The default ice nucleation scheme for cirrus clouds (below -35°C) in CAM5 follows the parameterization developed by Liu and Penner (2005) (hereafter LP) and was implemented in CAM3 by Liu et al. (2007) and later in CAM5 by Gettelman et al. (2010). The LP parameterization treats the competition between homogenous freezing on sulphate haze droplets and heterogeneous nucleation on dust as well as other IN. We also tested the ice nucleation parameterization by Barahona and Nenes (2009) (hereafter BN). In this study, we used both parameterizations. The BN parameterization has the flexibility to use different water accommodation coefficients and different ice nucleation parameterizations for heterogeneous nucleation including those in Meyers et al. (1992), Phillips et al. (2007) and Phillips et al. (2008) as well as the classical-nucleation-theory (CNT) (see Table 1 in Barahona and Nenes (2009)). The LP parameterization used the CNT based IN mechanism only and a fixed water accommodation coefficient equal to 0.1. To facilitate the comparison between the two parameterizations, we chose to use the CNT based IN mechanism in BN. In both ice nucleation parameterizations, up to 100% of the potential IN are allowed to freeze when criteria for temperatures and supersaturations are met. The results from the LP

parameterization are very similar to the results from the BN parameterization when the water vapour accommodation coefficient is set to 0.1. So we only present the results from the BN parameterization here.

The IMPACT module runs in parallel with the default CAM5 aerosol module (MAM3) in CAM5 (Zhou and Penner 2014). Aerosols simulated by the IMPACT module do not interact with any physical processes in CAM5 except in cirrus clouds (below -35 °C). In the ice nucleation parameterization sulphate particles and heterogeneous IN predicted by IMPACT replace those predicted by MAM3. The performance of the offline IMPACT model driven by CAM5 meteorological fields was previously evaluated by Zhou et al. (2012a, 2012b) and was in good agreement with observations. The overall characteristics of the performance of the coupled IMPACT module within CAM5 are similar to this offline version. We present simulations using two versions of IMPACT, the basic version without secondary organic aerosols (SOA) and the version that includes SOA. The basic version simulates a total of 17 externally mixed aerosol types and/or size bins: 3 sizes representing the number and mass of pure sulphate aerosols (i.e. nucleation, Aitken and accumulation modes), 3 types of fossil/bio-fuel soot that depend on its hygroscopicity or the amount of sulphate on the soot particles, 2 aircraft soot modes (pre-activated in contrails or not), 1 biomass soot mode, 4 dust sizes, and 4 sea salt sizes. All these aerosols may mix with sulphate through condensation and coagulation processes or through sulphate formation in cloud drops. Thus, for all non-sulphate aerosols we also track the amount of sulphate mass coated on them. The SOA version includes the volatile organic compound (VOC) oxidation scheme implemented in *Lin et al.* (2012, 2014). It has approximately 129 separate gas-phase compounds (depending on which chemical oxidation scheme is used). It uses a chemical mechanism that includes both gas phase and aqueous or liquid phase production of SOA. Specifically, Glyoxal and methylglyoxal are dissolved into cloud and aqueous sulfate to form SOA, and some SOA is formed through the reactive uptake of epoxides on aqueous sulfate. Twenty different semi-volatile organic compounds (SVOCs), mainly consisting of organic nitrates and peroxides that are formed from gas phase VOC oxidations, are partitioned into the aerosol phase. In addition, when present within the aerosol phase, the SVOCs form oligomers using a simplified scheme (*Lin et al.*, 2012). In total, in addition to the 17 aerosol species in the basic version of IMPACT described above, the *Lin et al.* (2014) version separately follows a total of 35 additional low-volatility SOA species.

2.2 Experiment Description

In the ice nucleation parameterization, we specify a single updraft velocity at each grid point. We used three different representations of the updraft: the grid resolved updraft velocity (WGRID), the updraft velocity derived from observed meso-scale temperature fluctuations as summarized by Gary (2006, 2008) (WGARY), and the updraft velocity based on the modelled sub-grid scale turbulent kinetic energy (WTKE). For each updraft representation, we used 4 different model set-ups, depending on whether heterogeneous nucleation (COMP), vapour deposition on pre-existing ice during ice nucleation (PRE), or SOA IN (SOA01) are included in the ice nucleation parameterization (COMP, COMP+SOA01, COMP+PRE and COMP+PRE+SOA01). Table 1 gives the definition of the set-ups for each updraft velocity category. In addition, for WGRID we added 2 other set-ups: a case with only homogeneous nucleation allowed (HOM) and a model set-up with vapour deposition on pre-existing ice during ice nucleation (HOM+PRE). Since we also vary the water vapour accommodation coefficient ($\alpha=0.1$ or $\alpha=1$), each set-up also includes a pair of simulations, one with $\alpha=0.1$ and one with $\alpha=1$. All cases use a horizontal resolution of $2.5^\circ \times 1.9^\circ$ and 30 vertical layers and are run for 6 years using year 2000 emissions. We chose to run the SOA capable version of the CAM/IMPACT model for only 2 years and to read-in the stored monthly averaged SOA fields from the second year for all cases, since the SOA capable version of the CAM/IMPACT model takes roughly 1.5 times more computer time than the basic version. The use of monthly averaged SOA fields does not significantly change the nature of the results. The output from the last 5 years of each simulation case is used in the analysis.

3 Results

3.1 Updraft velocities and SOA IN numbers

The updraft velocity plays a crucial role in ice nucleation. It determines how fast the RH_i can grow and thus determines whether the RH_i reaches the threshold for ice nucleation to occur after vapour deposition on newly formed ice begins. Figure 1a shows the probability density functions (PDFs) determined by sampling the updraft used during nucleation over tropical grids. Model results are sampled every 3 hours from all grid points between 30°S to 30°N and below 87hPa. The PDFs for the three different updraft velocities used here are shown for two different temperature ranges (185K-205K and 205K-225K). Results are from the COMP case in each updraft velocity category with $\alpha=0.1$. The grid resolved large scale

updraft velocity (WGRID) shows both negative and positive values varying between about - 0.05 m s⁻¹ to 0.15 m s⁻¹. The magnitude of WGRID decreases as the temperature decreases (from 205K-225K to 185K-205K) or when the altitude increases. WGARY is the updraft velocity derived from the observed meso-scale temperature fluctuations, δT , and is a function of altitude, topography, season, and latitude (Gary 2006, 2008). The observed temperature fluctuations were converted to sub-grid scale vertical velocities using

$$WGARY \text{ (m s}^{-1}\text{)} = 0.23 \delta T \text{ (K)}$$

following Kärcher and Burkhardt (2008) (also see Wang and Penner 2010 and Wang et al. 2014). WGARY varies from 0.05 m s⁻¹ to 0.15 m s⁻¹ and shows increased magnitudes as the temperature decreases with altitude. This increase is proportional to $p^{-0.4}$ (p is the pressure, see equation 3 in Gary (2008)) and is similar to the increase caused by the increase in the wave amplitudes required to conserve wave energy when the air density decreases with altitude. WTKE is the updraft velocity calculated from the modelled sub-grid turbulent kinetic energy (TKE) following Morrison and Pinto (2005):

$$WTKE = \sqrt{\frac{2}{3} TKE}$$

The TKE is diagnosed from CAM5's moist turbulence scheme which simulates cloud-radiation-turbulence interactions in an explicit way and is operating in any layer above as well as within PBL as long as the moist Richardson number is larger than a critical value, 0.19. WTKE has the largest range of the three representations. It has a spike near zero which occurs when strong turbulence/convection is absent in a grid. The remaining portion of the PDF has a wide range from 0 to 2 m s⁻¹. Large updraft velocities, such as those at the higher end of this range produced from convection in the tropics, are accompanied by homogeneous freezing as we show later. Previously, an artificial upper limit of 0.2 m s⁻¹ was used for WTKE in ice nucleation studies using the CAM5 model (Gettelman et al. 2010, 2012; Liu et al. 2012b; Zhang et al. 2013) to better reproduce observed in-cloud ice number concentrations. This upper limit was removed by Shi et al. (2015) after adding vapour deposition on pre-existing ice during ice nucleation. Here we also use the predicted updraft based on the TKE without any upper limit. We note that Shi et al. (2015) also limited the fraction of each grid cell that was allowed to undergo homogeneous freezing. Here, we do not add this constraint.

During in-cloud ice nucleation, the updraft velocity (W) acts to increase the relative humidity by cooling the air parcel through adiabatic expansion while pre-existing ice particles act to decrease the relative humidity by consuming any water vapour above ice saturation. So mathematically, one can combine the effects of pre-existing ice particles and those from the cooling caused by the updraft velocity. This is equivalent to the use of a reduced updraft velocity while ignoring vapour deposition on pre-existing ice particles. This reduced updraft velocity is termed the effective updraft velocity (Kärcher et al. 2006; Shi et al. 2015). Figure 1b shows the PDFs of the three different updraft velocities and their effective updraft velocities in the temperature range 185K-205K sampled from grid points that only experience homogenous freezing. The effective updraft velocities shift to the left towards the smaller values. The effective WGRID PDF now only shows positive values since homogeneous freezing only occurs in grid boxes with updrafts that are positive and are cooling. Although the effective WTKE is significantly reduced, it still has a large fraction with values larger than 0.2 m s^{-1} .

In addition to the important role that the updraft velocity plays in ice nucleation, the concentrations of heterogeneous IN also play an important role by determining the competition between heterogeneous nucleation and homogeneous freezing. However, our understanding of which aerosol particles may serve as heterogeneous IN is still limited (Hoose and Möhler, 2012) and even the importance of heterogeneous nucleation for the cold temperature regime (i.e., $T < 235 \text{ K}$) is still under discussion and not clear at the moment. The ability of different types of aerosols acting as IN was investigated in laboratory experiments (e.g., the formation of ice crystals on glassy particles). However, *in situ* measurements of heterogeneous IN are difficult. Furthermore, the existence of glassy particles within the atmosphere has not been established by *in situ* measurements. The field study by Cziczo et al. (2013) showed that mineral dust dominates most measurements of the residual particles in ice crystals. Another field study by Pratt et al. (2009) showed that ice-crystal residues from an aircraft measurement at high altitudes over Wyoming are comprised mostly of biological particles (~33%) and mineral dust (~50%) with some minor contribution from soot (~4%), salt (~4%) and organic carbon/nitrate (~9%). Moreover, the measurements in Cziczo et al. (2013) are mainly from convective regions in the subtropics and are certainly not representative for the whole upper troposphere, especially not for mid or high latitude conditions. Also the relevance of biological particles at cirrus level is not clear, since Pratt et al. (2009) could provide only one flight at about 7 kilometres (i.e. at temperatures $T > 240 \text{ K}$),

which is also not representative for the whole upper troposphere. Lab studies show that activated fractions of Asian and Saharan desert dust can range from ~5–10% at -20 °C to 20–40% at temperatures colder than -40 °C (Field et al. 2006). In this study we assumed that 10% of the total dust number can act as IN which is similar to the fractions suggested by Zhang et al. (2013) and Wang et al. (2014). For primary carbonaceous aerosols, we assume 0.1% of hydrophilic fossil fuel soot, 0.05% of hydrophobic fossil fuel soot (Koehler et al., 2009) and 0.1% of total biomass burning soot (Möhler et al. 2005) are able to act as heterogeneous IN. For SOA, we lumped together all 35 SOA compounds together and assumed that 0.1% of the total SOA could act as IN, similar to the fraction of biomass burning soot.

Figure 2 shows the annual zonal mean sulphate aerosol number concentration above 500 hPa in the Aitken and accumulation modes which are the number of particles able to freeze homogeneously. The number concentrations for different heterogeneous IN are also shown. The simulated sulphate number in the Aitken and accumulation modes (fig. 2a) is of the order of 100 cm^{-3} in the tropical upper troposphere. The total IN without SOA (fig. 2b) ranges from 0.5 to 30 L^{-1} in the upper troposphere. They are dominated by dust IN (fig. 2d) with a minor contribution from biomass burning soot (fig. 2e) below the tropopause. The contribution from fossil/bio fuel soot is even smaller and is largely negligible above 150 hPa. The number concentration of 0.1% of SOA, which we treat here as IN, ranges 1 to 30 L^{-1} in upper troposphere (fig. 2c) and is about 2-5 times larger than the total background IN number without SOA above 200 hPa, except in the dust source and outflow regions near north Africa (not shown).

3.2 Results from WGRID cases

In this section, we examine the effect from water vapour deposition on pre-existing ice particles on ice crystal number concentrations when the grid resolved updraft velocity (WGRID) is used in the ice nucleation parameterization. We also examine the effect of including SOA as IN and of varying the water vapour accommodation coefficient. The use of the large-scale updraft velocity during ice nucleation is based on the parcel model study by Spichtinger and Krämer (2013). They showed that the superposition of large-scale updrafts and fast gravity waves would limit the ice nucleation time duration and thus the ice number. They showed that about 80% of the observed ice spectrum could be explained by homogenous freezing while the remaining 20% stem from heterogeneous and homogeneous freezing occurring within the same environment, and suggested that their parcel model results

could be reproduced using only the large-scale updraft velocity. Here we test this theory by using the large-scale grid resolved updraft velocity in the ice nucleation parameterization in CAM5.

Figure 3 shows the simulated in-cloud ice number concentrations as a function of temperature from the WGRID cases. The top panel shows the results from the homogeneous freezing only cases and bottom panel shows the results from the homogeneous freezing/heterogeneous nucleation competition cases. The left and right panels show the results using two different water vapour accommodation coefficients ($\alpha=0.1$ and 1). The background blue shade shows the 25%-75% percentiles of observed in-cloud ice number concentrations compiled by Krämer et al. (2009). The solid curves show the 50% percentiles of simulated ice number concentrations for each 1K bin and the error bars show the 25%-75% percentiles. The model results were sampled every 3 hours from 30 S to 75 N over tropical, mid-latitude and Arctic regions which include the observation locations reported in Krämer et al. (2009). Fig. 3a shows that the HOM case overestimates the ice number concentrations by more than one order of magnitude in cirrus clouds at temperatures less than 205K but agrees better with observations in the temperature range from 205K to 220K. When the effect of vapour deposition onto pre-existing ice is included, the effective WGRID ($0-5 \text{ cm s}^{-1}$) is smaller than the original WGRID ($0-15 \text{ cm s}^{-1}$) for the grids with homogeneous freezing only (see Fig. 1b). Since a smaller updraft velocity translates into a slower increase of RH_i with time, fewer newly formed ice particles from homogeneous freezing are needed to reverse the growth of RH_i and thus stall the further formation of particles from homogeneous freezing. In fact, if the number of pre-existing ice particles is large enough, homogeneous freezing may not even occur. As a result, the ice number concentration in the HOM+PRE case (blue curve) is substantially smaller than that from the HOM case, especially at lower temperatures (more than one order of magnitude). This case matches the observations of ice number concentration pretty well at temperatures less than 205K, but underestimates concentrations at temperatures higher than 205K. Fig. 3b shows the results using a larger water vapour accommodation coefficient ($\alpha=1$). Since ice particles grow faster with the larger water vapour accommodation coefficient, the RH_i grows more slowly. So fewer ice particles are formed. For the HOM case, the ice number concentrations are much smaller at lower temperatures (compare black curves in Figure 3a and 3b). Case HOM+PRE (blue curves) also shows fewer ice particles but the difference between the case with $\alpha=0.1$ and 1.0 is relatively smaller.

Fig 3c shows the results from the cases that include the competition between homogeneous and heterogeneous nucleation. Compared to the HOM case in Fig 3a, the COMP case in Fig 3c shows smaller ice number concentrations, which is expected since the competition from heterogeneous nucleation, which can occur at lower RH_i, reduces the occurrence frequencies of homogeneous freezing. The much larger concentrations of homogeneous freezing haze particles (see Fig. 2a) typically allow more ice to form than heterogeneous nucleation. When 0.1% of SOA number is added as IN (case COMP+SOA01), there is a further reduction in the ice number concentration, especially at lower temperatures. But at higher temperatures (T>205K) the change is relatively smaller. This is because at higher temperatures (T>205K) ice grows faster than at lower temperatures thus the effect of any additional IN (SOA IN here) is diminished. When vapour deposition onto pre-existing ice is included (case COMP+PRE), the effect on ice number is much larger than the case for the addition of SOA IN. The predicted ice number concentrations in this case are of the order of 10 L⁻¹, which is comparable to the SOA IN number (about 10 L⁻¹ as shown in Fig. 2c). The SOA IN require an RH_i of about 120% to nucleate and start to consume the water vapour, while the pre-existing ice particles, if present, can start to consume the excess water vapour as long as the RH_i is above 100%. So the pre-existing ice particles are more effective at reducing the RH_i and suppressing ice nucleation by homogeneous and/or heterogeneous nucleation. In case COMP+PRE, since the effective WGRID is small, homogeneous freezing is almost completely suppressed. Further adding SOA IN to case COMP+PRE+SOA01 only decreases the ice number at the coldest temperatures (<195K). When a larger water vapor accommodation coefficient ($\alpha=1$) is used (Fig 3d), SOA IN are more effective at reducing the ice number at the coldest temperatures (see the pink curve at T<195K in Fig 3d) but become less important when vapour deposition onto pre-existing ice is included.

All in all, for cases using the large-scale grid resolved updraft velocity, as long as vapour deposition onto pre-existing ice is included, both the homogeneous freezing only case (HOM) and the competition cases (COMP) can produce in-cloud ice numbers in good agreement with the observations in the TTL cirrus clouds at temperatures less than 205K. If vapour deposition onto pre-existing ice during ice nucleation is not considered, then a larger water vapour accommodation coefficient ($\alpha=1$) together with SOA as IN can also lead to a good agreement with observations. One caveat regarding the above results is that since the dynamical region studied in Spichtinger and Krämer (2013) was for very special conditions (namely it is characterized by very low vertical updrafts (< 2 cm s⁻¹), low temperatures (T<205K) and

strong stratification (i.e. high Brunt-Väisälä frequency)), the use of the large-scale grid resolved updraft velocity may not be valid for weaker stratifications or when WGRID is not small enough.

3.3 Results from WGARY cases

Figure 4 shows the results from the cases that include homogeneous/heterogeneous competition using WGARY as the sub-grid scale updraft velocity in the ice nucleation parameterization. Results from the COMP case compare well with the observations in warm cirrus clouds in the temperature range from 205K to 220K for both water vapour accommodation coefficients. However, these cases overestimate number concentrations at temperatures less than 205K. Similar to the results in Fig. 3, including vapour deposition onto pre-existing ice can effectively reduce the in-cloud ice number concentrations. This leads to underestimated ice number concentrations in warmer cirrus. But unlike the results from the WGRID cases in Fig. 3, for this intermediate range updraft velocity (WGARY from 0.05-0.15 m s^{-1} in Fig. 1), the inclusion of vapour deposition onto pre-existing ice alone is not able to explain the observed low ice number concentrations in cold cirrus clouds ($T < 205\text{K}$). Adding SOA IN (red curves in Fig. 4) further reduces the in-cloud ice number concentrations at the lowest temperatures especially if $\alpha=1$. Adding SOA without including pre-existing ice (pink curves in Fig. 4) is not very effective at the lowest temperatures unless $\alpha=1$. The best prediction of ice number concentrations in cold cirrus clouds ($T < 205\text{K}$) is from case COMP+PRE+SOA01 (red curve in Fig. 4b) when the effects from the pre-existing ice particles, a larger water vapor accommodation coefficient ($\alpha=1$) and SOA IN are all included. At higher temperatures ($T > 210\text{K}$) there is a slight increase of ice number concentration when adding SOA in the pre-existing ice case, which suggests heterogeneous nucleation already dominates in this temperature regime, so that the addition of SOA IN acts to increase ice numbers.

3.4 Results from WTKE cases

Figure 5 shows the results from cases with both heterogeneous and homogenous nucleation (COMP) when the updraft velocity (WTKE) is based on the sub-grid scale turbulent kinetic energy. As WTKE is on average much higher than the other two velocity cases, the COMP cases without vapour deposition onto pre-existing ice overestimate the ice numbers substantially for both water vapor accommodation coefficients. Adding SOA IN has

almost no effect on the simulated ice number concentrations except at higher temperatures around 220K (pink curve in Fig. 5a). The critical IN number needed to suppress homogeneous freezing increases with decreased temperature and increased updraft velocities. This suggests that when WTKE is used, the addition of 0.1% of the total SOA as IN is not large enough to reach this critical IN number (except at some of the temperatures higher than 215K) (see pink curve in Fig. 5a). If 1% of the total SOA is allowed to act as IN, then there are significant decreases in the ice number concentrations at temperatures above 205K (see pink curves in Fig. S1). But the effect is still small at the lowest temperatures. When vapor deposition onto pre-existing ice is included, the WTKE is reduced but is still quite large compared to WGARY (see Fig. 1b). The simulated ice numbers from the COMP+PRE case are reduced by almost one order of magnitude and compare well with observations in cirrus clouds at temperatures warmer than 205K for both water vapour accommodation coefficients. Since the effective WTKE is smaller than the original WTKE, SOA IN are able to reduce some of the occurrences of homogeneous freezing at temperatures as low as 205K (see red curve in Fig. 5a). But overall the effect from the added SOA IN is small and not effective in reducing the ice number concentration for these larger updraft velocities. Similar results have been reported in a geoengineering study by Penner et al. (2015) when WTKE is used and 0.1% or 0.5% of total SOA is added as IN (see their Fig. 2).

4 Conclusion and Discussion

In this study, we examined the effect from three different updraft velocities and two different water vapor accommodation coefficients ($\alpha=0.1$ or 1) used in ice nucleation parameterizations. We also examined the effect of including vapour deposition onto pre-existing ice particles during ice nucleation and the effect of including SOA as heterogeneous IN. The different simulations were compared to observed in-cloud ice number concentrations in cirrus clouds. The simulated in-cloud ice number is shown to strongly depend on the magnitude of the updraft velocity since this determines the occurrence frequency of homogeneous freezing. Inclusion of vapour deposition onto pre-existing ice during nucleation or increasing the water vapor accommodation coefficient (from 0.1 to 1) can both effectively reduce the simulated ice numbers. The effect from SOA acting as IN is more complex since it depends on the background ice nucleation mechanism and whether or not the effect of pre-existing ice is included. Overall, SOA IN are most effective at suppressing homogeneous

freezing and thus reducing ice numbers when updraft velocities are intermediate in magnitude (e.g. WGARY from 0.05-0.15 m s⁻¹). Including the effect of pre-existing ice reduces the effect of SOA IN. For small updraft velocities (e.g. WGRID), SOA IN are effective at reducing ice numbers only at lower temperatures. For large updraft velocities (e.g. WTKE), SOA IN only show a small effect at higher temperatures.

Here is a summary of the set-ups for different updraft velocities needed to produce ice number concentrations in-line with observations at temperatures less than 205K:

- 1) For the small grid resolved updraft velocities (i.e., case WGRID where W is typically < 0.1 m s⁻¹), using either homogenous freezing only or including the competition between homogeneous and heterogeneous nucleation in the ice nucleation parameterization is able to produce the observed lower ice numbers when vapour deposition onto pre-existing ice particles is considered. When vapour deposition onto pre-existing ice particles is not considered, then a larger water vapour accommodation coefficient ($\alpha=1$) and SOA IN are both needed to produce the observed lower ice numbers.
- 2) For intermediate velocities (e.g., WGARY with W varying from 0.05-0.15 m s⁻¹), the effects from vapour deposition onto pre-existing ice particles, a larger water vapour accommodation coefficient ($\alpha=1$), and SOA IN are all needed to produce the observed lower ice numbers.
- 3) For the larger updraft velocities (such as those found in WTKE which vary up to 2 m s⁻¹), all set-ups overestimate the in-cloud ice numbers.

Thus, from our study, one can only use WGRID and WGARY to reproduce in-cloud ice numbers in-line with observations at temperatures less than 205K. But these simulations underestimate the ice number at temperatures higher than 205K. On the other hand, even though no set-up for WTKE is able to reproduce in-cloud ice numbers in-line with observations at temperatures less than 205K, the results agree best with observations at temperatures higher than 205K. No simple tuning of the ice nucleation parameters or set-up can form ice number concentrations that fit both temperature ranges. The obvious issue is that ice numbers from the model and the observations have nearly opposite temperature dependence slopes (i.e., decreased ice number with increased temperature seen from models vs. increased ice number with increased temperature seen from observations), a point noted previously using parcel model studies (Murphy 2014). The slope seen from the model results

is a fundamental consequence of slower growth rate of ice particles and less water vapour available at lower temperatures. The only way to reverse the slope would be if some parameters, such as IN concentrations or sub-grid updraft velocity, were themselves functions of temperature. It is possible that CAM5 may overestimate the TKE in the upper troposphere at temperatures less than 205K, but an analysis of this is beyond the scope of this paper. When we use WGRID at temperatures lower than 205K and WTKE at temperatures higher than 205K, we are able to reverse the slope and the simulated ice number concentrations fit the observations well in both temperature ranges (see Fig. 6a). But this choice of updraft velocity lacks any theory or observational support. It might be that we could only apply the proposal by Spichtinger and Krämer (2013) of using the large-scale updraft in the ice nucleation parameterization at temperatures lower than 205K but not at temperatures higher than 205K. The dynamic conditions near the top of troposphere may favour a combination of a slow persistent large-scale updraft velocity and short gravity waves which satisfy the special situation described by Spichtinger and Krämer (2013) in which the ice number formed from the short gravity waves is limited; while at lower altitudes, short gravity waves effect may not be limited due to higher large-scale updraft velocities. Another possibility might be that SOA number concentrations only become glassy and act as IN at temperatures less than 205K. However, while this model setup allows us to improve the prediction of crystal concentrations below 205K, it does not produce a reversed slope. Since the dynamical regime studied in Spichtinger and Krämer (2013) is characterized by a strong increasing stratification (i.e. high Brunt-Väisälä frequency) which coincides with the decreasing low temperatures ($T < 205\text{K}$) near the TTL, a more physical criterion would be using the modelled Brunt-Väisälä frequency (N) to split the different regimes (WGRID vs. WTKE). Fig. 6b shows the simulated in-cloud ice numbers when using WGRID for $N \leq 0.1 \text{ s}^{-1}$ and WTKE for $N > 0.1 \text{ s}^{-1}$. The critical value, $N = 0.1 \text{ s}^{-1}$, occurs around the altitude where the annually and zonally averaged $T = 205\text{K}$ in the tropics. The simulated in-cloud ice number at $T < 205\text{K}$ improves but not as much as that in Fig 6a in which the critical value of T (205K) is used. This is likely because the altitude at which $N = 0.1 \text{ s}^{-1}$ does not necessarily coincide with the altitude at which $T = 205\text{K}$ at any given time step in the model.

Acknowledgements

1 This work was supported by the NSF under grants AGS-0946739 and AGS-1540954. We
2 acknowledge high-performance computing support from Yellowstone
3 (<http://n2t.net/ark:/85065/d7wd3xhc>) provided by NCAR's Computational and Information
4 Systems Laboratory and sponsored by the National Science Foundation.

5

References

- Abbatt, J. P. D., Benz, S., Cziczo, D. J., Kanji, Z., Lohmann, U., and Möhler, O.: Solid ammonium sulfate aerosols as ice nuclei: a pathway for cirrus cloud formation, *Science*, 313, 1770–1773, doi:10.1126/science.1129726, 2006.
- Barahona, D. and Nenes, A.: Parameterization of cirrus formation in large scale models: Homogenous nucleation, *J. Geophys. Res.*, 113, D11211, doi:10.1029/2007JD009355, 2008.
- Barahona, D. and Nenes, A.: Parameterizing the competition between homogeneous and heterogeneous freezing in ice cloud formation – polydisperse ice nuclei, *Atmos. Chem. Phys.*, 9, 5933–5948, doi:10.5194/acp-9-5933-2009, 2009.
- Barahona, D. and Nenes, A.: Dynamical states of low temperature cirrus, *Atmos. Chem. Phys.*, 11, 3757–3771, doi:10.5194/acp-11-3757-2011, 2011.
- Chen, T., Rossow, W. B., and Zhang, Y.: Radiative effects of cloud-type variations. *J. Clim.* 13, 264–286, 2000.
- Cziczo, D. J., Froyd, K. D., Hoose, C., Jensen, E. J., Diao, M., Zondlo, M. A., Smith, J. B., Twohy, C. H., and Murphy, D. M.: Clarifying the Dominant Sources and Mechanisms of Cirrus Cloud Formation, *Science*, 340, 1320–1324, doi:10.1126/science.1234145, 2013.
- Diao, M., Zondlo, M. A., Heymsfield, A. J., Beaton, S. P., and Rogers, D. C.: Evolution of ice crystal regions on the microscale based on in situ observations, *Geophys. Res. Lett.*, 40, 3473–3478, doi:10.1002/grl.50665, 2013.
- Diao, M., Zondlo, M. A., Heymsfield, A. J., and Beaton, S. P.: Hemispheric comparison of cirrus cloud evolution using in situ measurements in HIAPER Pole-to-Pole Observations, *Geophys. Res. Lett.*, 41, 4090–4099, doi:10.1002/2014GL059873, 2014.
- Diao, M., Beaton, S. P., Pan, L. L., Homeyer, C. R., Honomichl, S., Bresch, J. F. and Bansemer A.: Distributions of ice supersaturation and ice crystals from airborne

- observations in relation to upper tropospheric dynamical boundaries, *J. Geophys. Res. Atmos.*, 120, 5101–5121, doi:10.1002/2015JD023139, 2015.
- Dinh, T., Podglajen, A., Hertzog, A., Legras, B., and Plougonven, R.: Effect of gravity wave temperature fluctuations on homogeneous ice nucleation in the tropical tropopause layer, *Atmos. Chem. Phys. Discuss.*, 15, 8771–8799, doi:10.5194/acpd-15-8771-2015, 2015.
- Field, P. R., Möhler, O., Connolly, P., Krämer, M., Cotton, R., Heymsfield, A. J., Saathoff, H., and Schnaiter, M.: Some ice nucleation characteristics of Asian and Saharan desert dust, *Atmos. Chem. Phys.*, 6, 2991–3006, doi:10.5194/acp-6-2991-2006, 2006.
- Gary, B. L.: Mesoscale temperature fluctuations in the stratosphere, *Atmos. Chem. Phys.*, 6, 4577–4589, doi:10.5194/acp-6-4577-2006, 2006.
- Gary, B. L.: Mesoscale temperature fluctuations in the Southern Hemisphere stratosphere, *Atmos. Chem. Phys.*, 8, 4677–4681, doi:10.5194/acp-8-4677-2008, 2008.
- Gettelman, A., Liu, X., Ghan, S. J., Morrison, H., Park, S., Conley, A. J., Klein, S. A., Boyle, J., Mitchell, D. L., and Li, J. L. F.: Global simulations of ice nucleation and ice supersaturation with an improved cloud scheme in the Community Atmosphere Model, *J. Geophys. Res.-Atmos.*, 115, D18216, doi:10.1029/2009jd013797, 2010.
- Gettelman, A., Liu, X., Barahona, D., Lohmann, U., and Chen, C.: Climate impacts of ice nucleation, *J. Geophys. Res.-Atmos.*, 117, D20201, doi:10.1029/2012jd017950, 2012.
- Hoose, C. and Möhler, O.: Heterogeneous ice nucleation on atmospheric aerosols: a review of results from laboratory experiments, *Atmos. Chem. Phys.*, 12, 9817–9854, doi:10.5194/acp-12-9817-2012, 2012.
- IPCC, 2013: Climate Change 2013: The Physical Science Basis. Contribution of Working Group I to the Fifth Assessment Report of the Intergovernmental Panel on Climate Change [Stocker, T.F., D. Qin, G.-K. Plattner, M. Tignor, S.K. Allen, J. Boschung, A. Nauels, Y. Xia, V. Bex and P.M. Midgley (eds.)]. Cambridge University Press, Cambridge, United Kingdom and New York, NY, USA, 1535 pp.

- 1 Jensen, E. J., Toon, O. B., Selkirk, H. B., Spinhirne, J. D., and Schoeberl, M. R.: On the
2 formation and persistence of subvisible cirrus clouds near the tropical tropopause,
3 J. Geophys. Res., 101, 21361–21375, 1996.
- 4 Jensen, E. J., Pfister, L., Bui, T.-P., Lawson, P., and Baumgardner, D.: Ice nucleation and
5 cloud microphysical properties in tropical tropopause layer cirrus, Atmos. Chem.
6 Phys., 10, 1369–1384, doi:10.5194/acp-10-1369-2010, 2010.
- 7 Jensen, E. J., Pfister, L., and Bui T. P.: Physical processes controlling ice concentrations
8 in cold cirrus near the tropical tropopause, J. Geophys. Res., 117, D11205,
9 doi:10.1029/2011JD017319, 2012.
- 10 Jensen, E. J., Diskin, G., Lawson, R. P., Lance, S., Bui, T. P., Hlavka, D., McGill, M.,
11 Pfister, L., Toon, O. B., and Gao, R.: Ice nucleation and dehydration in the
12 Tropical Tropopause Layer, P. Natl. Acad. Sci., 110, 2041–2046,
13 doi:10.1073/pnas.1217104110, 2013.
- 14 K ärcher, B. and Str öm, J.: The roles of dynamical variability and aerosols in cirrus cloud
15 formation, Atmos. Chem. Phys., 3, 823–838, doi:10.5194/acp-3-823-2003, 2003.
- 16 K ärcher, B., Hendricks, J., and Lohmann, U.: Physically based parameterization of cirrus
17 cloud formation for use in global atmospheric models, J. Geophys. Res., 111,
18 D01205, doi: 10.1029/2005JD006219, 2006.
- 19 K ärcher, B. and Burkhardt, U.: A cirrus cloud scheme for general circulation models,
20 Quart. J. Roy. Meteor. Soc., 134, 1439–1461, doi:10.1002/Qj.301, 2008.
- 21 Kay, J. E., and Wood, R.: Timescale analysis of aerosol sensitivity during homogeneous
22 freezing and implications for upper tropospheric water vapor budgets, Geophys.
23 Res. Lett., 35, L10809, doi:10.1029/2007gl032628, 2008.
- 24 Koehler, K. A., DeMott, P. J., Kreidenweis, S. M., Popovicheva, O. B., Petters, M. D.,
25 Carrico, C. M., Kireeva, E. D., Khokhlovac, T. D., and Shonijac, N. K.: Cloud
26 condensation nuclei and ice nucleation activity of hydrophobic and hydrophilic
27 soot particles, Phys. Chem. Chem. Phys., 11, 7906–7920, doi:10.1039/b905334b,
28 2009.
- 29 Koop, T., Luo, B., Tsias, A., and Peter, T.: Water activity as the determinant for
30 homogeneous ice nucleation in aqueous solutions, Nature, 406, 611–614, 2000.

- 1 Kr ämer, M., Schiller, C., Afchine, A., Bauer, R., Gensch, I., Mangold, A., Schlicht, S.,
2 Spelten, N., Sitnikov, N., Borrmann, S., de Reus, M., and Spichtinger, P.: Ice
3 supersaturations and cirrus cloud crystal numbers, *Atmos. Chem. Phys.*, 9, 3505-
4 3522, doi:10.5194/acp-9-3505-2009, 2009.
- 5 Kuebbeler, M., Lohmann, U., Hendricks, J., and Krächer, B.: Dust ice nuclei effects on
6 cirrus clouds, *Atmos. Chem. Phys.*, 14, 3027-3046, doi:10.5194/acp-14-3027-2014, 2014.
- 7 Lin, G., Penner, J. E., Sillman, S., Taraborrelli, D., and Lelieveld, J.: Global modeling of
8 SOA formation from dicarbonyls, epoxides, organic nitrates and peroxides,
9 *Atmos. Chem. Phys.*, 12, 4743-4774, doi:10.5194/acp-12-4743-2012, 2012.
- 10 Lin, G., Sillman, S., Penner, J. E., and Ito, A.: Global modeling of SOA: the use of
11 different mechanisms for aqueous-phase formation, *Atmos. Chem. Phys.*, 14,
12 5451-5475, doi:10.5194/acp-14-5451-2014, 2014.
- 13 Liu, X. and Penner, J. E.: Ice nucleation parameterization for a global model,
14 *Meteorologische Zeitschrift*, 14(4), 499–514, 2005.
- 15 Liu, X., Penner, J. E., Ghan, S. J., and Wang, M.: Inclusion of ice microphysics in the
16 NCAR community atmospheric model version 3 (CAM3), *J. Climate*, 20, 4526–
17 4547, doi: 10.1175/JCLI4264.1, 2007.
- 18 Liu, X., Easter, R. C., Ghan, S. J., Zaveri, R., Rasch, P., Shi, X., Lamarque, J.-F.,
19 Gettelman, A., Morrison, H., Vitt, F., Conley, A., Park, S., Neale, R., Hannay, C.,
20 Ekman, A. M. L., Hess, P., Mahowald, N., Collins, W., Iacono, M. J., Bretherton,
21 C. S., Flanner, M. G., and Mitchell, D.: Toward a minimal representation of
22 aerosols in climate models: description and evaluation in the Community
23 Atmosphere Model CAM5, *Geosci. Model Dev.*, 5, 709-739, doi:10.5194/gmd-5-
24 709-2012, 2012a.
- 25 Liu, X., Shi, X., Zhang, K., Jensen, E. J., Gettelman, A., Barahona, D., Nenes, A., and
26 Lawson, P.: Sensitivity studies of dust ice nuclei effect on cirrus clouds with the
27 Community Atmosphere Model CAM5, *Atmos. Chem. Phys.*, 12, 12061-12079,
28 doi:10.5194/acp-12-12061-2012, 2012b.
- 29 Magee, N., Moyle, A. M., and Lamb, D.: Experimental determination of the deposition
30 coefficient of small cirrus-like ice crystals near -50 °C, *Geophys. Res. Lett.*, 33,
31 L17813, doi:10.1029/2006GL026665, 2006.

- 1 Meyers, M. P., DeMott, P. J., and Cotton, R.: New primary ice nucleation
2 parameterization in an explicit cloud model, *J. Appl. Meteorol.*, 31, 708–721,
3 1992.
- 4 Möhler, O., Büttner, S., Linke, C., Schnaiter, M., Saathoff, H., Stetzer, O., Wagner, R.,
5 Krämer, M., Mangold, A., Ebert, V., and Schurath, U.: Effect of sulfuric acid
6 coating on heterogeneous ice nucleation by soot aerosol particles, *J. Geophys.*
7 *Res.*, 110, D11210, doi:10.1029/2004JD005169, 2005.
- 8 Morrison, H., and Gettelman A., A new two-moment bulk stratiform cloud microphysics
9 scheme in the Community Atmosphere Model, version 3 (CAM3). Part I:
10 Description and numerical tests. *Journal of Climate*, 21, 3642–3659,
11 doi:10.1175/2008JCLI2105.1, 2008.
- 12 Morrison, H., and Pinto J. O.: Mesoscale modeling of springtime arctic mixed-phase
13 stratiform clouds using a new two-moment bulk microphysics scheme, *J. Atmos.*
14 *Sci.*, 62, 3683–3704, 2005.
- 15 Murphy, D. M.: Rare temperature histories and cirrus ice number density in a parcel and a
16 one-dimensional model, *Atmos. Chem. Phys.*, 14, 13013–13022, doi:10.5194/acp-
17 14-13013-2014, 2014.
- 18 Murray, B., Wilson, T. W., Dobbie, S., Cui, Z., Al-Jumur, S. M. R. K., Möhler, O.,
19 Schnaiter, M., Wagner, R., Benz, S., Niemand, M., Saathoff, H., Ebert, V.,
20 Wagner, S., and Krächer, B.: Heterogeneous nucleation of ice particles on glassy
21 aerosols under cirrus conditions, *Nat. Geosci.*, 3, 233–237,
22 doi:10.1038/NGEO817, 2010.
- 23 Neale, R. B., Gettelman, A., Park, S., Conley, A. J., Kinnison, D., Marsh, D., Smith, A.
24 K., Vitt, F., Morrison, H., Cameron-Smith, P., Collins, W. D., Iacono, M. J.,
25 Easter, R. C., Liu, X., and Taylor, M. A.: Description of the NCAR Community
26 Atmosphere Model (CAM 5.0), NCAR Tech. Note NCAR/TN-485CSTR, Natl.
27 Cent. for Atmos. Res, Boulder, Co, 289 pp., 2012.
- 28 Penner, J. E., Zhou, C. and Liu, X.: Can cirrus cloud seeding be used for geoengineering?,
29 *Geophys. Res. Lett.*, 42, 8775–8782, doi:10.1002/2015GL065992, 2015.

- 1 Phillips, V. T. J., Donner, L. J., and Garner, S. T.: Nucleation processes in deep
2 convection simulated by a cloud-system-resolving model with double-moment
3 bulk microphysics, *J. Atmos. Sci.*, 64, 738–761, doi:10.1175/JAS3869.1, 2007.
- 4 Phillips, V. T. J., DeMott, P. J., and Andronache, C.: An empirical parameterization of
5 heterogeneous ice nucleation for multiple chemical species of aerosol, *J. Atmos.*
6 *Sci.*, 65, 2757–2783, doi:10.1175/2007JAS2546.1, 2008.
- 7 Pratt, K., DeMott, P., French, J., Wang, Z., Westphal, D., Heyms-field, A., Twohy, C.,
8 Prenni, A., and Prather, K.: In situ detection of biological particles in cloud ice-
9 crystals, *Nature Geosci.*, 2, 398–401, 2009.
- 10 Pruppacher, H. R. and Klett, J. D.: *Microphysics of Clouds and Precipitation*,
11 *Atmospheric and Oceanographic Sciences Library*, Kluwer Academic Publishers,
12 Dordrecht, The Netherlands, 1997.
- 13 Ramanathan, V. and Collins, W.: Thermodynamic regulation of ocean warming by cirrus
14 clouds deduced from observations of the 1987 El-Nino, *Nature*, 351, 27–32, 1991.
- 15 Rogers, D. C., DeMott, P. J., Kreidenweis, S. M. and Chen, Y.: Measurements of ice
16 nucleating aerosols during SUCCESS, *Geophys. Res. Lett.*, 25, 1383–1386,
17 doi:10.1029/97GL03478, 1998.
- 18 Rossow, W. B. and Schiffer, R. A.: Advances in understanding clouds from ISCCP, *Bull.*
19 *Amer. Meteor. Soc.*, 80, 2261–2287, 1999.
- 20 Sassen, K., Wang Z., and Liu, D.: Global distribution of cirrus clouds from
21 CloudSat/Cloud-Aerosol Lidar and Infrared Pathfinder Satellite Observations
22 (CALIPSO) measurements, *J. Geophys. Res.*, 113, D00A12,
23 doi:10.1029/2008JD009972, 2008.
- 24 Shi, X., Liu, X., and Zhang, K.: Effects of pre-existing ice crystals on cirrus clouds and
25 comparison between different ice nucleation parameterizations with the
26 Community Atmosphere Model (CAM5), *Atmos. Chem. Phys.*, 15, 1503-1520,
27 doi:10.5194/acp-15-1503-2015, 2015.
- 28 Skrotzki, J., Connolly, P., Schnaiter, M., Saathoff, H., Möhler, O., Wagner, R., Niemand,
29 M., Ebert, V., and Leisner, T.: The accommodation coefficient of water molecules

- on ice – cirrus cloud studies at the AIDA simulation chamber, *Atmos. Chem. Phys.*, 13, 4451-4466, doi:10.5194/acp-13-4451-2013, 2013.
- Spichtinger, P. and Gierens, K. M.: Modelling of cirrus clouds – Part 2: Competition of different nucleation mechanisms, *Atmos. Chem. Phys.*, 9, 2319-2334, doi:10.5194/acp-9-2319-2009, 2009.
- Spichtinger, P. and Kräner, M.: Tropical tropopause ice clouds: a dynamic approach to the mystery of low crystal numbers, *Atmos. Chem. Phys.*, 13, 9801-9818, doi:10.5194/acp-13-9801-2013, 2013.
- Stubenrauch, C. J., Cros, S., Guignard, A., and Lamquin, N.: A 6-year global cloud climatology from the Atmospheric InfraRed Sounder AIRS and a statistical analysis in synergy with CALIPSO and CloudSat, *Atmos. Chem. Phys.*, 10, 7197-7214, doi:10.5194/acp-10-7197-2010, 2010. Wang, M. and Penner, J. E.: Cirrus clouds in a global climate model with a statistical cirrus cloud scheme, *Atmos. Chem. Phys.*, 10, 5449-5474, doi:10.5194/acp-10-5449-2010, 2010.
- Wang, M., Liu, X., Zhang K., and Comstock J. M.: Aerosol effects on cirrus through ice nucleation in the Community Atmosphere Model CAM5 with a statistical cirrus scheme, *J. Adv. Model. Earth Syst.*, 6, 756–776, doi:10.1002/2014MS000339, 2014.
- Wang, P. H., Minnis, P., McCormick, M. P., Kent, G. S., and Skeens, K. M.: A 6-year climatology of cloud occurrence frequency from stratospheric aerosol and gas experiment II observations (1985-1990), *J. Geophys. Res.*, 101, 29407–29429, 1996.
- Wylie, D. P. and Menzel, W. P.: Eight years of high cloud statistics using HIRS, *J. Climate*, 12, 170–184, 1999.
- Zhang, K., Liu, X., Wang, M., Comstock, J. M., Mitchell, D. L., Mishra, S., and Mace, G. G.: Evaluating and constraining ice cloud parameterizations in CAM5 using aircraft measurements from the SPARTICUS campaign, *Atmos. Chem. Phys.*, 13, 4963-4982, doi:10.5194/acp-13-4963-2013, 2013.
- Zhou, C., and Penner J. E.: Aircraft soot indirect effect on large-scale cirrus clouds: Is the indirect forcing by aircraft soot positive or negative?, *J. Geophys. Res. Atmos.*, 119, doi:10.1002/2014JD021914, 2014.

1 Zhou, C., Penner, J. E., Flanner, M. G., Bisiaux, M. M., Edwards, R. and McConnell J.
2 R.:Transport of black carbon to polar regions: Sensitivity and forcing by black
3 carbon, Geophys. Res. Lett., 39, L22804, doi:10.1029/2012GL053388, 2012b.
4 Zhou, C., Penner, J. E., Ming, Y., and Huang, X. L.: Aerosol forcing based on CAM5 and
5 AM3 meteorological fields, Atmos. Chem. Phys., 12, 9629-9652, doi:10.5194/acp-
6 12-9629-2012, 2012a.

1 Table 1. Description of the experiments.

Case name	Case description
HOM [*]	Only homogeneous freezing in the ice nucleation parameterization.
HOM+PRE [*]	Only homogeneous freezing in the ice nucleation parameterization; pre-existing ice effect in the ice nucleation parameterization.
COMP	Competition between homogeneous freezing and heterogeneous nucleation.
COMP+SOA01	Competition between homogeneous freezing and heterogeneous nucleation; 0.1% of SOA acting as heterogeneous IN.
COMP+PRE	Competition between homogeneous freezing and heterogeneous nucleation; pre-existing ice effect in the ice nucleation parameterization.
COMP+PRE+SOA01	Competition between homogeneous freezing and heterogeneous nucleation; pre-existing ice effect in the ice nucleation parameterization; 0.1% of SOA acting as heterogeneous IN.

2 ^{*} Case HOM and HOM+PRE are for WGRID only.

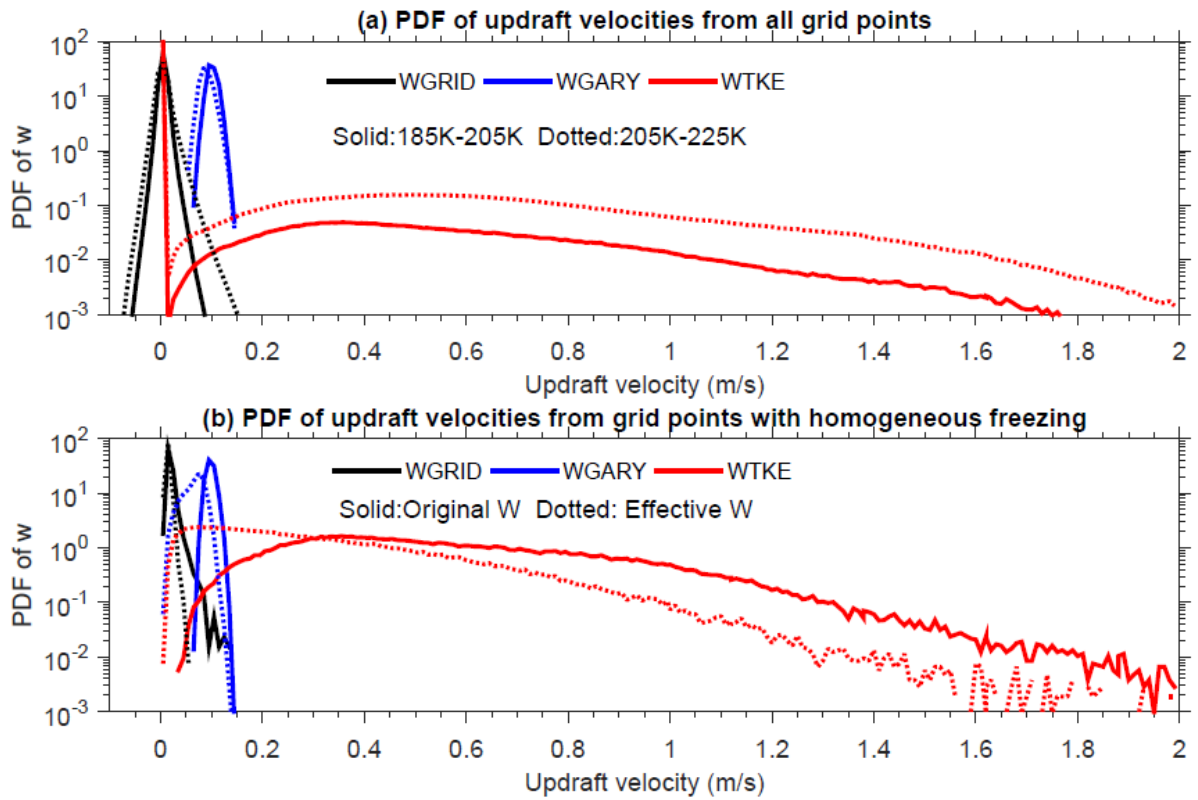


Figure 1 (a) Probability density functions (PDFs) of updraft velocity for three different representations (black: large-scale W , blue: meso-scale W from Gary 2006, 2008, red: TKE based subgrid W) from all grid points in two temperature ranges. (b) Probability density functions of updraft velocity for the three different updraft velocity representations from grid points with homogenous freezing only in the temperature range 185K-205K. Solid curves are the original W and dotted curves are the effective W after accounting for vapour deposition onto pre-existing ice. Model results are sampled every 3 hour below 87hPa.

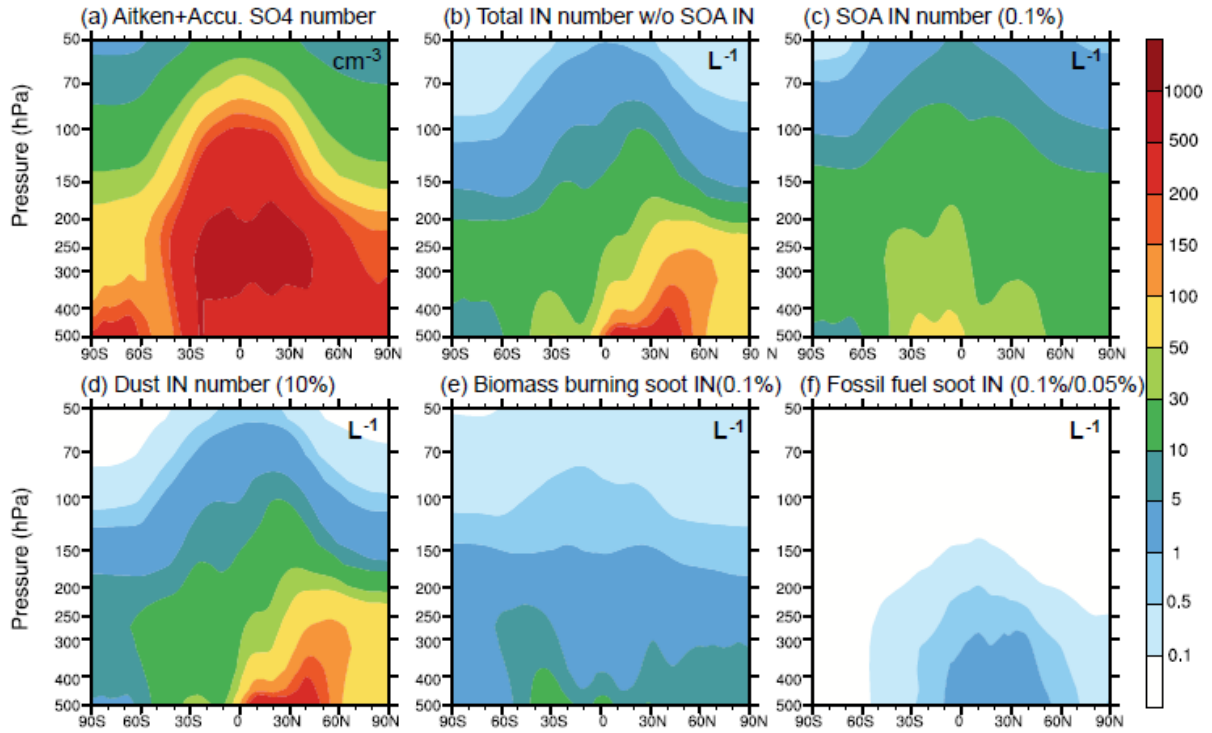


Figure 2 a) Aitken and accumulation mode sulfate number (cm^{-3}). b) Total background heterogeneous IN number (L^{-1}) without SOA IN: i.e. the sum of panels d, e, and f. c) SOA IN number (L^{-1}): 0.1% of the total SOA number. d) Dust IN number (L^{-1}): 10% of the total dust number. e) Biomass burning soot IN number (L^{-1}): 0.1% of total biomass burning soot number. f) Fossil fuel soot IN number (L^{-1}): 0.1% of hydrophilic fossil fuel soot and 0.05% of hydrophobic fossil fuel soot.

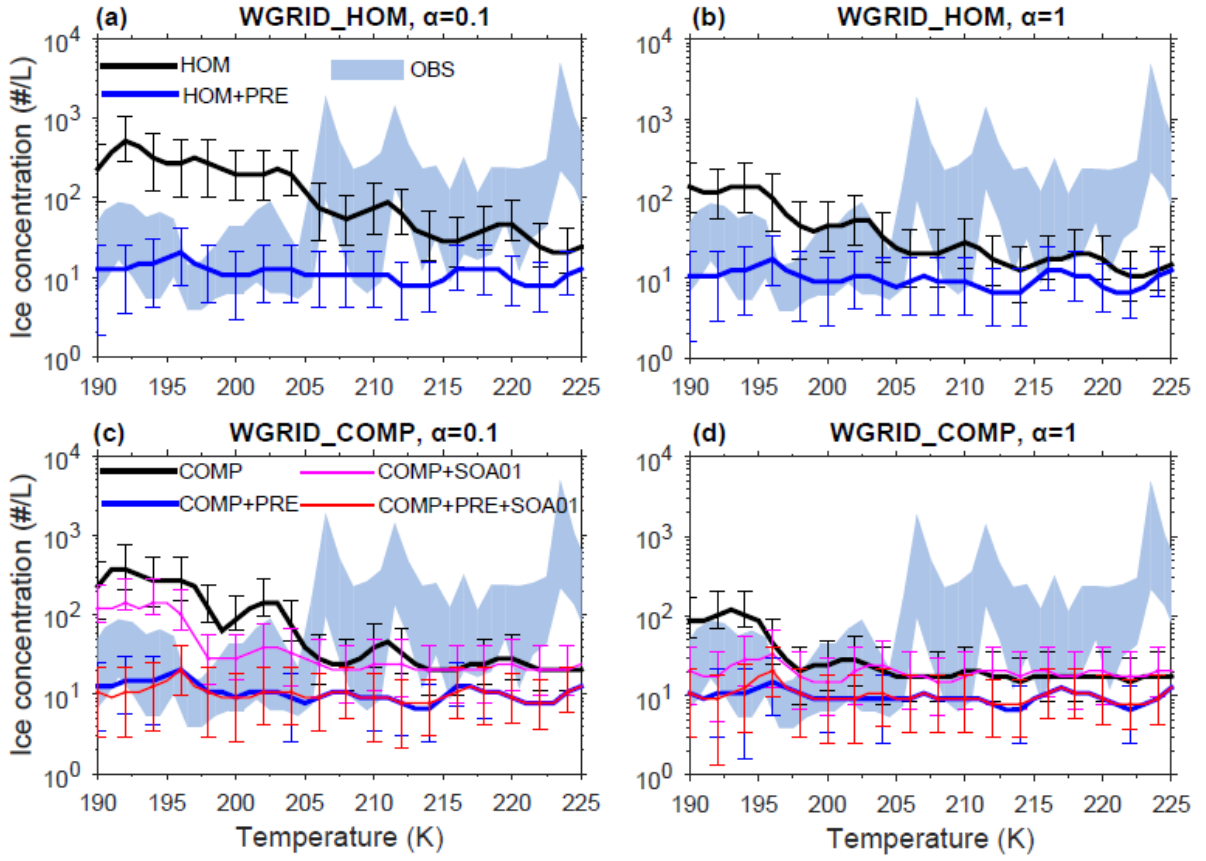


Figure 3 In-cloud ice crystal number concentration (#/L) versus temperature from cases using the grid resolved updraft velocity (WGRID) in the ice nucleation parameterization. Solid lines show the 50% percentile values for each 1K bin. Error bars show the 25%-75% percentiles. Background shaded regions show the 25%-75% percentiles from observations compiled by Krämer et al. (2009). Upper panel shows the results from the homogeneous freezing only cases and bottom panel shows the results from the competition cases. Left panel shows the results from cases with water vapor accommodation coefficient $\alpha = 0.1$. Right panel shows the results from cases with water vapor accommodation coefficient $\alpha = 1$. Model results are sampled every 3 hours from 30 S to 75 N over tropical, mid-latitude and Arctic regions which includes the observation locations reported in Krämer et al. (2009).

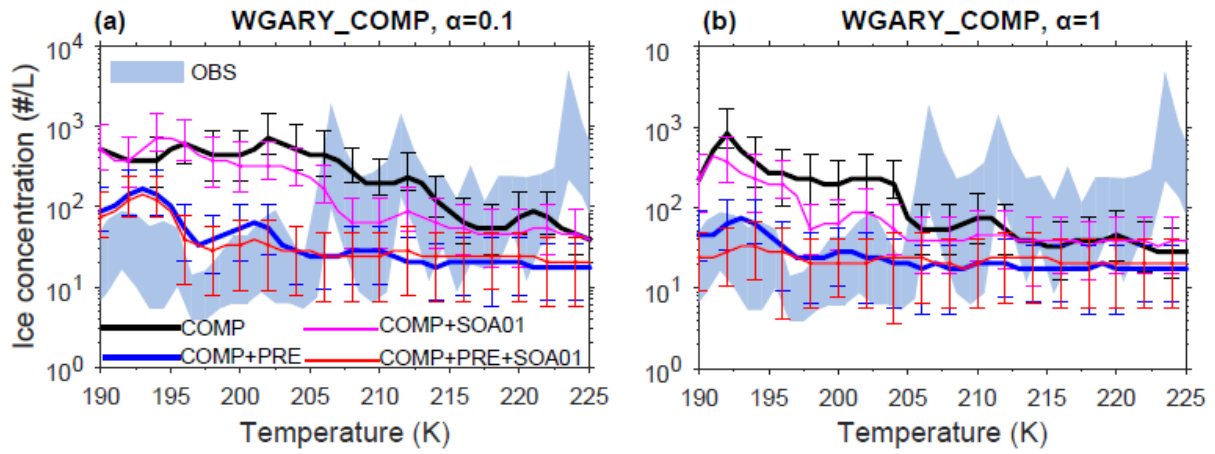


Figure 4 Same as Figure 3 (c) and (d) except the updraft velocity (WGARY) derived from the observed meso-scale temperature fluctuations from Gary (2006, 2008) was used in the ice nucleation parameterization.

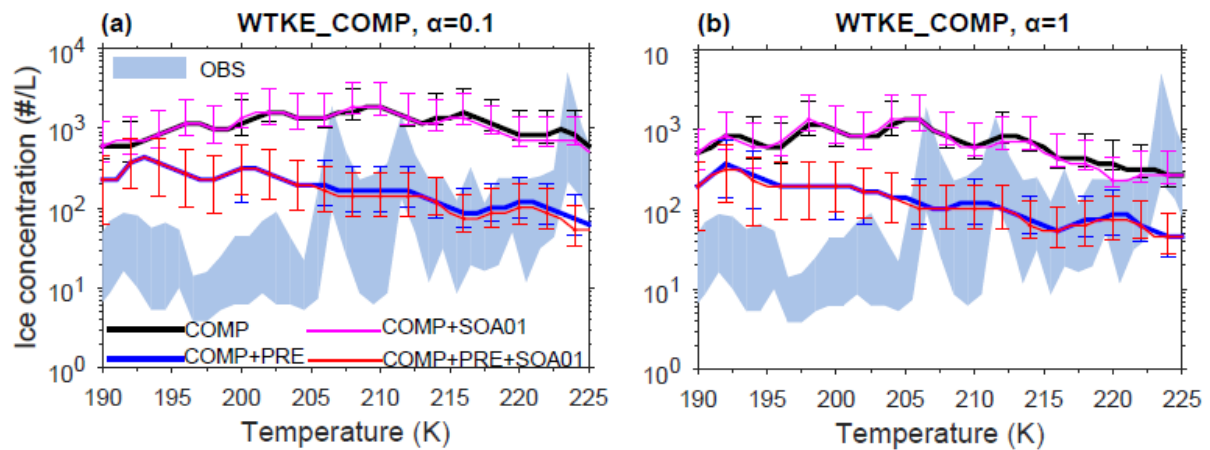


Figure 5 Same as Figure 3 (c) and (d) except the sub-grid scale turbulent kinetic energy based updraft velocity (WTKE) was used in the ice nucleation parameterization.

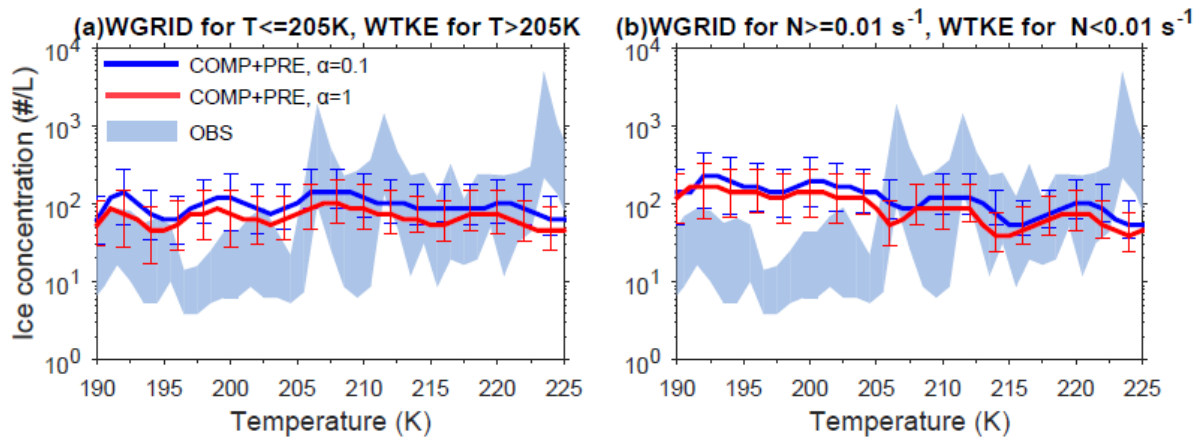


Figure 6 In-cloud ice crystal number concentration (#/L) versus temperature from COMP+PRE cases with a mixed use of WGRID and WTKE based on a critical temperature or Brunt-Väisälä frequency. (left) WGRID for $T \leq 205\text{K}$ and WTKE for $T > 205\text{K}$; (right) WGRID for the Brunt-Väisälä frequency $N \geq 0.01 \text{ s}^{-1}$ and WTKE for $N < 0.01 \text{ s}^{-1}$. Blue curves is from the case with water vapor accommodation coefficient $\alpha = 0.1$ and the red curves are from the case with water vapor accommodation coefficient $\alpha = 1$.

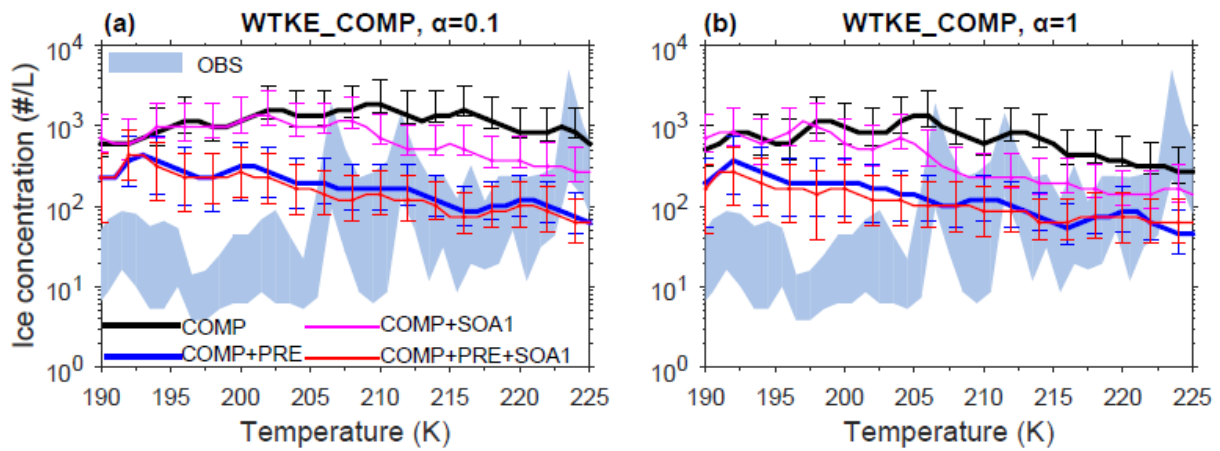


Figure S1 Same as Figure 5 except 1% of total SOA acting as IN.